# Deuterium Isotope Effect on the Atomic Alignment Dependence in the Reaction of Oriented Ar ($^3P_2$) with $(CH_3CN)_2$ and $(CD_3CN)_2$ Dimers

**T. Matsumura, H. Ohoyama,* D. Watanabe, K. Yasuda, and T. Kasai**

*Department of Chemistry, Graduate School of Science, Osaka University, Toyonaka, Osaka 560-0043, Japan*

*Received: April 9, 2007; In Final Form: May 16, 2007*

The effect of atomic alignment on CN ($B^2\Sigma^+$) formation has been studied in the reaction of oriented Ar ($^3P_2$) with $(CX_3CN)_2$ (X = H, D). The reaction cross-section for each magnetic $M_J'$ substate in the collision frame $\sigma^{|M_J'|}_{H(D),d}$ relative to the cross-section $\sigma^0_{H,m}$ in the $CH_3CN$ reaction was determined to be $\sigma^0_{H,d}/\sigma^{|1|}_{H,d}/\sigma^{|2|}_{H,d}/\sigma^0_{D,d}/\sigma^{|1|}_{D,d}:/\sigma^{|2|}_{D,d} = 0.87/1.00/0.98/1.58/1.93/1.78$. A notable deuterium isotope effect was observed. In contrast with the monomer reactions, a significant decrease of $\sigma^0_{H(D),d}$ relative to the other cross-sections of $\sigma^{|M_J'|}_{H(D),d}$ was observed.

## 1. Introduction

The energy transfer process is a very important fundamental process for chemical reactions such as the initial steps in the photosynthetic process.[1] The reaction of a metastable rare gas with a small molecule has been widely studied as the benchmark system,[2−6] and it is known that these processes are affected by orbital overlap. The importance of molecular orientation linked with the spatial distribution of the molecular orbital has been reported by our laboratory.[7−12] On the other hand, little is known about the steric aspect for the atomic orientation in multiplet systems.

Recently, we directly studied the steric effect in the Ar ($^3P_2$) + $N_2 \rightarrow N_2$ (C, $^3\Pi_u$) + Ar reaction by using an oriented Ar ($^3P_2$, $M_J = 2$) beam.[13] A significant alignment dependence on the atomic orbital and the little contribution of the rank 4 moment has been observed. The electron spin was found to have little effect on the dynamics as assumed by the Percival-Seaton hypothesis.[14] On the other hand, we observed a significant contribution of the rank 4 moment ($a_4$) in the dimer reactions of Ar ($^3P_2$) + $(N_2O)_2$, $(H_2O)_2$[15] contrary to the Percival-Seaton hypothesis. This result indicates the importance of the spin interaction between the unpaired inner orbital and the outer extended orbital in the course of energy transfer dynamics of triplet systems.

The reaction of Ar ($^3P_2$) + $CH_3CN$ ($CD_3CN$) is one of the most widely studied reaction systems to date.[16−21] The comparison of the cross-section of a few Å$^2$ for CN (B) formation with 160 Å$^2$ for the total quenching cross-section of Ar* by $CH_3CN$ gives the low branching fraction for CN (B) formation.[19−21] These results are parallel to the small quantum yield for the production of CN (B) observed in the VUV photodissociation, and they support the idea that CN (B) formation is competitive with other fast exit channels.[22] The main channel of the title reaction is estimated to be the H-elimination.

For these reactions, we studied the molecular orientation dependence for the CN ($B^2\Sigma^+$) formation by using the oriented $CH_3CN$ ($CD_3CN$) beam.[16,17] From the large stereo-anisotropy observed in the CN ($B^2\Sigma^+$) formation for the reaction with oriented $CH_3CN$, we suggested the important contribution of the $7a_1$ orbital, which is localized at the CN group. In addition, we observed the deuterium isotope effect on the molecular orientation dependence and on the cross-section.[17] We attributed the effects of the deuterium isotope on the cross-section to the dissociation dynamics from the excited states because the energy transfer probability depends only on the electronic term and has no isotope effect. To explain the incremental change of the reaction probability by the deuteration of $CH_3CN$, we argued that the deuteration of the molecule reduces the CD vibrational frequency and makes the competition of D-elimination less effective than CN (B) formation after the energy transfer has occurred. In addition, the incremental change of the reaction probability by the deuteration of $CH_3CN$ showed a nearly isotropic behavior on molecular orientation. From these results, we suggested that the additional process was attributed to the reaction relevant to the 2e molecular orbital that has the spatial distribution spreading over the sideways direction.[17] Recently, we studied the effect of atomic alignment on CN ($B^2\Sigma^+$) formation in the oriented Ar ($^3P_2$) + $CX_3CN$ (X = H, D) reaction.[23] On the basis of the effects of the deuterium isotope on the atomic alignment effect, we tested the earlier proposal that the reaction of the 2e orbital was responsible for the increase in cross-section with deuteration, and we suggested that the expectation of the static anisotropy for the orbital overlap efficiency between the 2e and 3p orbitals is inadequate to explain the deuterium isotope effect on both the atomic alignment and the molecular orientation dependence. In addition, some configurational correlations between the atomic alignment and the molecular orientation were proposed.[23]

In the present study, the effects of dimer formation on both the atomic alignment effect and the deuterium isotope effect are studied for the CN ($B^2\Sigma^+$) formation in the reaction of oriented Ar ($^3P_2$) with $(CX_3CN)_2$ (X = H, D). The reaction cross-sections for each magnetic $M_J'$ sub-state in the collision frame, $\sigma^{|M_J'|}_{H(D),d}$ are determined. A significant decrease of $\sigma^0_{H(D),d}$ relative to the other $\sigma^{|M_J'|}_{H(D),d}$ is observed in contrast with the monomer reaction.

## 2. Experimental Procedures

Details of the experimental apparatus and the procedure were described elsewhere,[13,15,23] and only an outline is given here. An almost pure Ar ($^3P_2$, $M_J = 2$) beam (more than 93%) was generated by using an inhomogeneous magnetic hexapole.[21] A $CX_3CN$ (X = H, D) beam was injected from a pulsed valve with a stagnation pressure range of 2−25 Torr. In the homogeneous magnetic orientation field B, the $M_J$ state-selected Ar ($^3P_2$, $M_J = 2$) beam collides with the $CX_3CN$ beam. The chemiluminescence of product CN (B) was measured as a

* To whom correspondence should be addressed. E-mail: Ohyama@chem.sci.osaka-u.ac.jp.

10.1021/jp0727446 CCC: $37.00 
Published on Web 07/04/2007

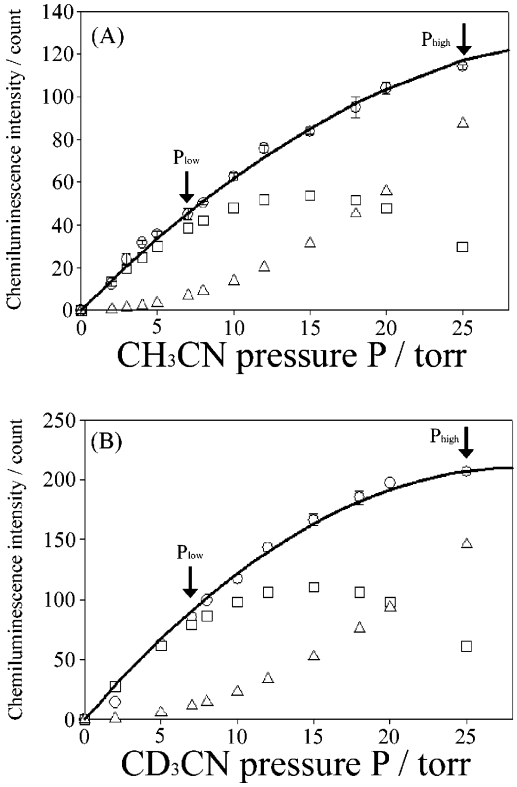


**Figure 1.** Stagnation pressure dependence of CN ($B^2\Sigma^+$) chemiluminescence intensity at $\Theta = 60°$ for the reactions (A) Ar ($^3P_2$) + $CH_3CN$ and (B) Ar ($^3P_2$) + $CD_3CN$. Experimental data (open circles). Each component is estimated by the fitting using eq 1 for monomer (squares) and dimer (triangles).

function of the direction of the magnetic orientation field in the laboratory frame (rotation angle $\Theta$). The magnetic orientation field B was rotated around the beam crossing point over the angle region $-45 \leq \Theta \leq 165°$ by an interval of 15°. The origin of $\Theta$ is the direction of the Ar beam axis. The chemiluminescence from the product CN (B) was selectively collected by a concave mirror and was detected by a cooled and magnetically shielded photomultiplier (Hamamatsu R943−02) mounted 30 cm from the beam crossing point through a suitable band-pass filter (HOYA U340 & $\lambda_C = 390$ nm). The signal from the photomultiplier was counted by a multichannel scaler (Stanford SR430).

## 3. Results

**3.1. Stagnation Pressure Dependence of Chemiluminescence Intensity.** To study the steric effect in the dimer reaction of $(CX_3CN)_2$ (X = H, D) with the oriented Ar ($^3P_2$), the stagnation pressure dependence of the CN ($B^2\Sigma^+$) chemiluminescence intensity was measured at an angle of $\Theta = 60°$. The stagnation pressure dependence is shown in Figure 1, panels A and B, for $CH_3CN$ and $CD_3CN$, respectively. In the low stagnation pressure, the chemiluminescence intensity appears to be linearly proportional to the stagnation pressure. This linear relationship indicates that the monomer is the only dominant species at low stagnation pressure. However, the linearity breaks down as the stagnation pressure increases. We attribute this nonlinearity to cluster formation. It is reasonable to consider that dimer formation is the dominant process of cluster formation at the present stagnation pressure region. Under this assumption, the pressure dependence can be written as shown in eq 1

$$I_{H(D)}(P) = \sigma_{H(D),m}(P - 2k_dP^2) + \sigma_{H(D),d}k_dP^2 \qquad (1)$$

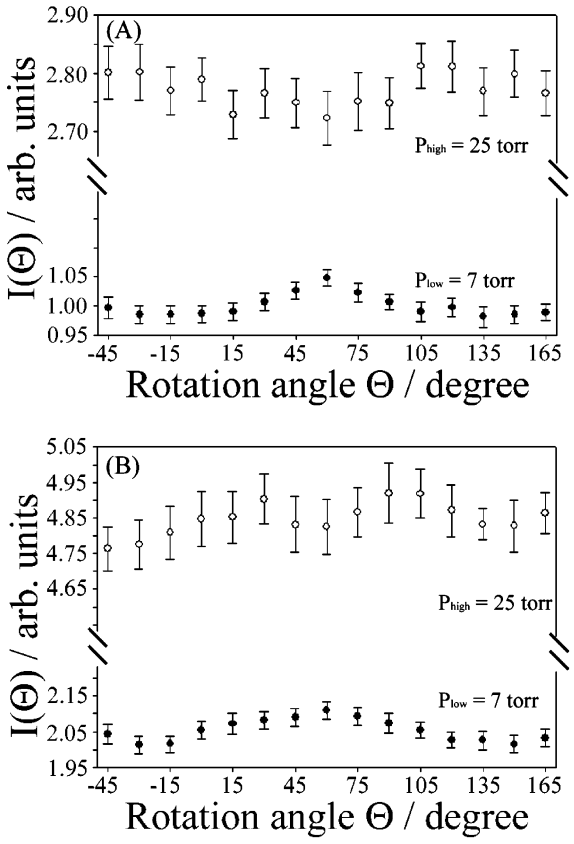


**Figure 2.** The chemiluminesence intensity of CN ($B^2\Sigma^+$) as a function of the orientation field direction $\Theta$ ($I_{H(D)}(\Theta)$) for the reaction of $CH_3CN$ (A) and $CD_3CN$ (B) at different two stagnation pressures. $P_{low}$ = 7 Torr (filled circles) and $P_{high}$ = 25 Torr (open circles).

**TABLE 1: The Coefficient Used in Equation 1 for Characterizing the Stagnation Pressure Dependence of the Chemiluminescence Intensity in the Ar ($^3P_2$) + $(CH_3CN)_n$ and Ar ($^3P_2$) + $(CD_3CN)_n$ Reactions**

| | $k_d$ (Torr$^{-1}$) | $\sigma_{H(D),d}/\sigma_{H(D),m}$ |
|---|---|---|
| $CH_3CN$ | $(1.7 \pm 0.1) \times 10^{-2}$ | $1.16 \pm 0.07$ |
| $CD_3CN$ | $(1.6 \pm 0.1) \times 10^{-2}$ | $0.95 \pm 0.03$ |

where $P$ is the stagnation pressure of $CX_3CN$, and the subscripts H and D designate $CH_3CN$ and $CD_3CN$, respectively. $\sigma_{H(D),m}$ and $\sigma_{H(D),d}$ are proportional to the reaction cross-section at the angle of $\Theta = 60°$ for $CX_3CN$ and $(CX_3CN)_2$, respectively, and $k_d$ is proportional to the rate constant for dimer formation. We can reproduce the experimental stagnation pressure dependence very well by using eq 1. Therefore, it is reasonable to assume that dimer formation is an initial and dominant process of cluster formation at this high stagnation pressure condition. $\sigma_{H(D),m}$, $\sigma_{H(D),d}$, and $k_d$ are determined as the parameters by fitting $I_{H(D)}(P)$ using eq 1, and they are summarized in Table 1. At the same time, the contributions of the monomer and the dimer can be estimated by this fitting procedure as a function of stagnation pressure, as shown in Figure 1.

**3.2. Steric Effect in the Ar ($^3P_2$) + $(CX_3CN)_2$ (X = H, D) Reaction.** The chemiluminescence intensity ($I_{H(D)}(\Theta)$) of the product CN ($B^2\Sigma^+$) in the Ar ($^3P_2$) + $(CX_3CN)_n$ (X = H, D) reaction was measured as a function of the orientation field direction $\Theta$ at low and high stagnation pressures ($P_{low}$ = 7 Torr and $P_{high}$ = 25 Torr). The $\Theta$-dependence at $P_{low}$ ($I^{low}_{H(D)}(\Theta)$) and $P_{high}$ ($I^{high}_{H(D)}(\Theta)$) are shown in Figure 2 panels A and B for $CH_3CN$ and $CD_3CN$, respectively. We can observe the notable difference between $I^{low}_{H(D)}(\Theta)$ and $I^{high}_{H(D)}(\Theta)$ due to dimer formation. To study the steric effect for the dimer reaction, the pure

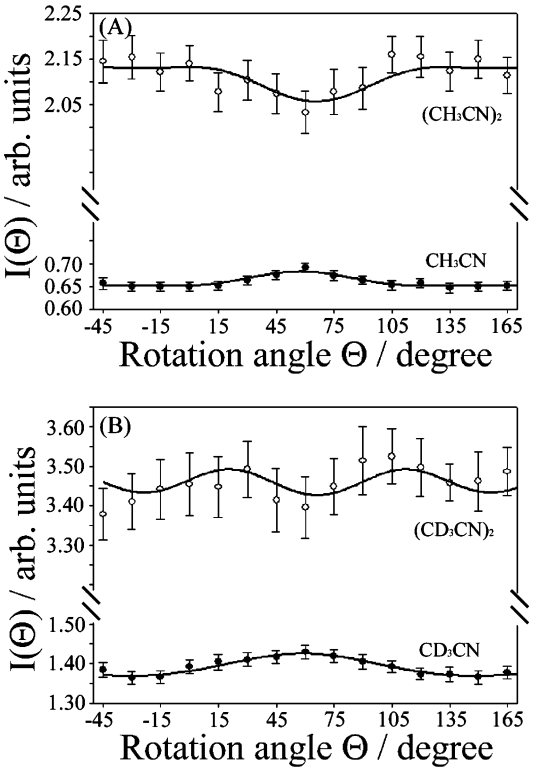


**Figure 3.** The deconvoluted chemiluminesence intensity of CN ($B^2\Sigma^+$) at $P_{high} = 25$ Torr. $I_{H(D),m(d)}(\Theta)$ for the monomer (filled circles) and the dimer (open circles) as a function of the orientation field direction $\Theta$ for the reaction of $CH_3CN$ (A) and $CD_3CN$ (B). The magnetic orientation field is parallel to the relative velocity vector at $\Theta = 58.0°$ (65.0°) in the Ar ($^3P_2$) + $CH_3CN$ ($CH_3CN$)$_2$ reaction and is parallel to the relative velocity vector at $\Theta = 58.4°$ (66.2°) in the Ar ($^3P_2$) + $CD_3CN$ ($CD_3CN$)$_2$ reaction.

dimer component in $I^{high}_{H(D)}(\Theta)$ must be extracted. We can estimate the contribution of the monomer component in $I^{high}_{H(D)}(\Theta)$ as the $I^{low}_{H(D)}(\Theta)$ weighted by the monomer intensity at $\Theta = 60°$ that can be estimated by eq 1. The deconvoluted $\Theta$-dependence of the chemiluminescence intensity for monomer ($I_{H(D),m}(\Theta)$) and for dimer ($I_{H(D),d}(\Theta)$) in $I^{high}_{H(D)}(\Theta)$ is shown in Figure 3.

## 4. Discussion

**4.1. $M'_J$-Dependent Cross-Section, $\sigma^{|M'_J|}$.** To extract the quantitative information on the steric effect in the dimer formation, we accommodate the evolution procedure based on an irreducible representation of the density matrix. The detail of the analytical procedures and the derivation of all of the algebra were reported elsewhere.[13,15]

The $\Theta$-dependence of the chemiluminescence intensity ($I(\Theta)$) can be simplified as the following equation by using the reaction cross-section for each magnetic $M'_J$ sub-state in the collision frame, $\sigma^{|M'_J|}_{H(D),d}$;

$$I_{H(D),m(d)}(\Theta) = \frac{1}{280}(39\sigma^0_{H(D),m(d)} + 88\sigma^{|1|}_{H(D),m(d)} + 153\sigma^{|2|}_{H(D),m(d)}) + \frac{1}{16}(-3\sigma^0_{H(D),m(d)} - 4\sigma^{|1|}_{H(D),m(d)} + 7\sigma^{|2|}_{H(D),m(d)})\langle\cos(2\theta)\rangle + \frac{1}{64}(3\sigma^0_{H(D),m(d)} - 4\sigma^{|1|}_{H(D),m(d)} + \sigma^{|2|}_{H(D),m(d)})\langle\cos(4\theta)\rangle \quad (2)$$

where the subscripts m and d designate monomer and dimer, respectively, $\theta$ is the angle between the relative velocity ($v_R$) and the direction of the orientation magnetic field ($B$). It is defined as $\theta \equiv \Theta_{v_R} - \Theta$ by using the direction of $v_R$ in the laboratory coordinate, $\Theta_{v_R}$. Because this angle has a distribution due to the misalignment caused by the velocity distribution of the $(CX_3CN)_n$ beam, we must use the cos $2n\theta$ factors averaged over the Maxwell−Boltzmann velocity distribution of the $(CX_3CN)_n$ beam at room temperature, $\langle\cos(2n(\Theta_{v_R} - \Theta))\rangle$. This equation is equivalent to the multipole moment form shown in eq 3;

$$I_{H(D),m(d)}(\Theta) = a_{0,H(D),m(d)} + a_{2,H(D),m(d)}\langle\cos 2(\Theta_{v_R} - \Theta)\rangle + a_{4,H(D),m(d)}\langle\cos 4(\Theta_{v_R} - \Theta)\rangle \quad (3)$$

The parameters $a_{n,H(D),m(d)}$ were determined by the fitting of $I_{H(D),m(d)}(\Theta)$ using eq 3. The relative cross-sections, $\alpha_{H(D),m(d)} \equiv \sigma^{|1|}_{H(D),m(d)}/\sigma^0_{H(D),m(d)}$ and $\beta_{H(D),m(d)} \equiv \sigma^{|2|}_{H(D),m(d)}/\sigma^0_{H(D),m(d)}$, can be derived from the experimental coefficient ratios of $a_{2,H(D),m(d)}/a_{0,H(D),m(d)}$ and $a_{4,H(D),m(d)}/a_{0,H(D),m(d)}$, respectively. They are summarized in Table 2. We observe a substantial contribution of the rank 4 moment ($a_4$) for the reaction of $(CX_3CN)_2$ that indicates a significant spin interaction between the unpaired inner orbital and the outer extended orbital.

By using the relative cross-sections $\alpha_{H(D),m(d)}$ and $\beta_{H(D),m(d)}$, $I_{H(D),m(d)}(\Theta)$ can be rewritten as shown in eq 4.

$$I_{H(D),m(d)}(\Theta) = \sigma^0_{H(D),m(d)}\left[\frac{1}{280}(39 + 88\beta_{H(D),m(d)} + 153\alpha_{H(D),m(d)}) + \frac{1}{16}(-3 - 4\beta_{H(D),m(d)} + 7\alpha_{H(D),m(d)})\langle\cos 2(\Theta_{v_R} - \Theta)\rangle + \frac{1}{64}(3 - 4\beta_{H(D),m(d)} + \alpha_{H(D),m(d)})\langle\cos 4(\Theta_{v_R} - \Theta)\rangle\right] \quad (4)$$

To comprehend the effect due to dimer formation, it is necessary to determine the relative cross-sections, $\sigma^{|M'_J|}_{H(D),m(d)}/\sigma^0_{H,m}$. The cross-sections $\sigma^0_{H,m}$, $\sigma^0_{H,d}$, $\sigma^0_{D,m}$, and $\sigma^0_{D,d}$ can be determined by comparing the cross-section of $\sigma_{H(D),m(d)}$ at $\Theta = 60°$, which is listed in Table 1 with the value of $I_{H(D),m(d)}$ ($\Theta = 60^0$) as

**TABLE 2: The Ratio of $a_{2,H(D),m(d)}/a_{0,H(D),m(d)}$ and $a_{4,H(D),m(d)}/a_{0,H(D),m(d)}$, and the Relative Cross-Section, $\alpha_{H(D),m(d)} \equiv \sigma^{|1|}_{H(D),m(d)}/\sigma^0_{H,m}$ and $\beta_{H(D),m(d)} \equiv \sigma^{|2|}_{H(D),m(d)}/\sigma^0_{H,m}$ for the Ar ($^3P_2$) + $(CX_3CN)_n$ (X = H, D) Reactions**

| | $CH_3CN$ | | $CD_3CN$ | |
|---|---|---|---|---|
| | monomer | dimer | monomer | dimer |
| $a_2/a_0$ | $-(2.4 \pm 0.3) \times 10^{-2}$ | $(1.7 \pm 0.3) \times 10^{-2}$ | $-(2.1 \pm 0.2) \times 10^{-2}$ | $(1.0 \pm 4.3) \times 10^{-3}$ |
| $a_4/a_0$ | $(1.1 \pm 0.4) \times 10^{-2}$ | $(-6.9 \pm 3.3) \times 10^{-3}$ | $(0.17 \pm 0.29) \times 10^{-2}$ | $(-1.0 \pm 0.5) \times 10^{-2}$ |
| $\alpha$ | $0.81 \pm 0.04$ | $1.00 \pm 0.13$ | $1.92 \pm 0.09$ | $1.93 \pm 0.40$ |
| $\beta$ | $0.84 \pm 0.03$ | $0.98 \pm 0.12$ | $1.87 \pm 0.07$ | $1.78 \pm 0.36$ |

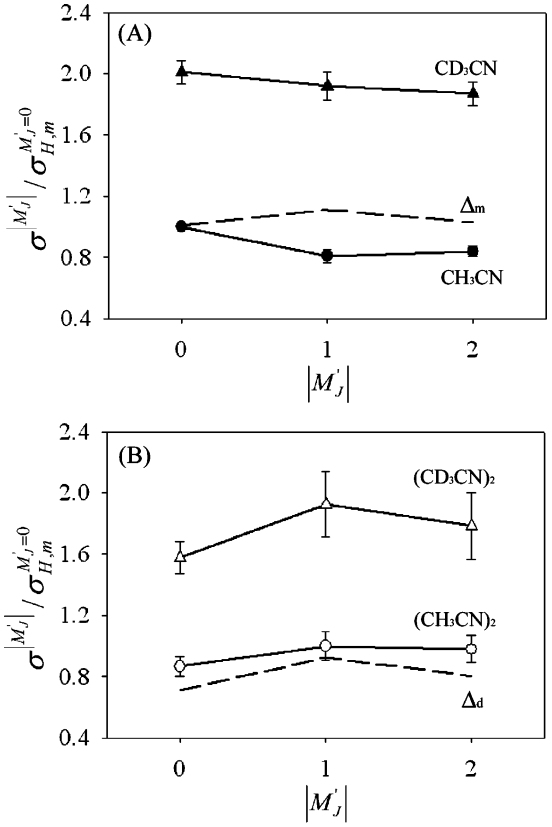


**Figure 4.** The $M_J'$-resolved relative cross-sections for (A) $CH_3CN$ (●), $CH_3CN$ (▲); (B) $(CH_3CN)_2$ (○), $(CD_3CN)_2$ (△). Dashed lines are the increment of the cross-section due to deuteration. (A) $\Delta_m^{|M_J'|}$ for $CH_3CN$, (B) $\Delta_d^{|M_J'|}$ for $(CH_3CN)_2$.

**TABLE 3: $M_J'$-Resolved Cross-Sections for the Ar ($^3P_2$) + $(CX_3CN)_n$ (X = H, D) Reactions**

| | $CH_3CN$ | | $CD_3CN$ | |
|---|---|---|---|---|
| | monomer | dimer | monomer | dimer |
| $\sigma^{M_J'=0}$ | 1.00 | 0.87 ± 0.10 | 2.01 ± 0.08 | 1.58 ± 0.31 |
| $\sigma^{\|M_J'\|=1}$ | 0.81 ± 0.04 | 1.00 ± 0.13 | 1.92 ± 0.09 | 1.93 ± 0.40 |
| $\sigma^{\|M_J\|=2}$ | 0.84 ± 0.03 | 0.98 ± 0.12 | 1.87 ± 0.07 | 1.78 ± 0.36 |

obtained from eq 4. As a result, the relative cross-sections are easily derived;

$$\sigma^0_{H,m}/\sigma^{|1|}_{H,m}/\sigma^{|2|}_{H,m}/\sigma^0_{D,m}/\sigma^{|1|}_{D,m}/\sigma^{|2|}_{D,m} = 1.00/0.81/0.84/2.01/1.92/1.87$$

$$\sigma^0_{H,d}/\sigma^{|1|}_{H,d}/\sigma^{|2|}_{H,d}/\sigma^0_{D,d}/\sigma^{|1|}_{D,d}/\sigma^{|2|}_{D,d} = 0.87/1.00/0.98/1.58/1.93/1.78$$

They are summarized in Table 3 and Figure 4. As a whole, the cross-section in the dimer reaction differs little from the monomer one. However, it is recognized that $\sigma^0_{H(D),d}$ was significantly smaller than $\sigma^0_{H(D),m}$.

To compare the deuterium isotope effect between the monomer and the dimer, for convenience, we separate the cross-section $\sigma^{|M_J'|}_{D,m(d)}$ into two parts;[17,23]

$$\sigma^{|M_J'|}_{D,m(d)} = \sigma^{|M_J'|}_{H,m(d)} + \Delta^{|M_J'|}_{m(d)}$$

where $\Delta_m^{|M_J'|}$ and $\Delta_d^{|M_J'|}$ are the increments of the cross-section by the deuteration of $CH_3CN$ and $(CH_3CN)_2$, respectively. They are determined as follows;

$$\Delta^0_m/\Delta^{|1|}_m/\Delta^{|2|}_m = 1.01/1.11/1.07$$

$$\Delta^0_d/\Delta^{|1|}_d/\Delta^{|2|}_d = 0.71/0.93/0.80$$

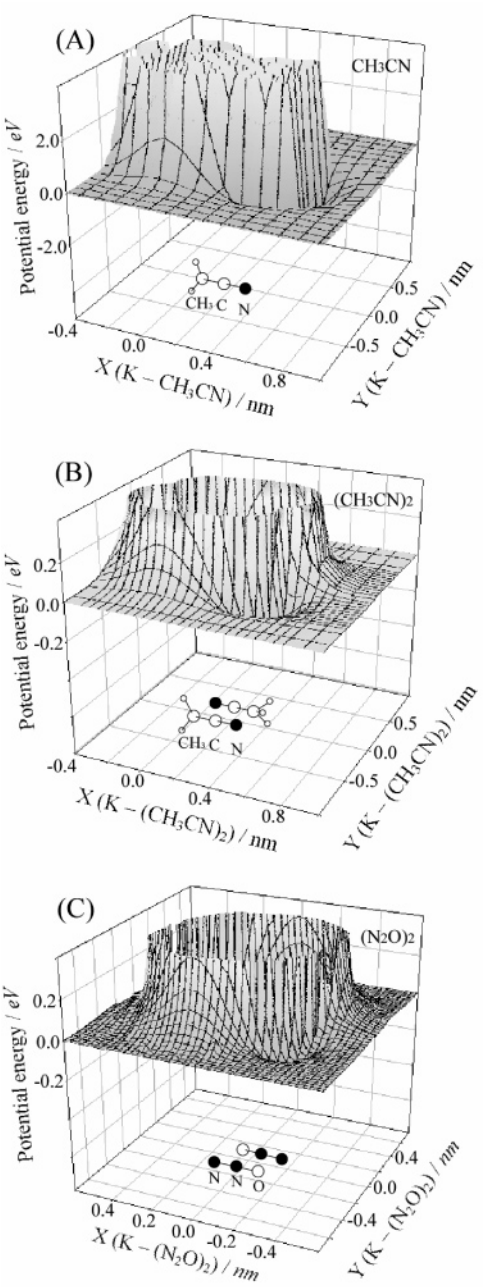


**Figure 5.** The model potential energy surface calculated by the GAUSSIAN 98 ab initio program package with the 6-31G basis set. (A) K + $(CH_3CN)_n$, (B) K + $(CH_3CN)_2$, and (C) K + $(N_2O)_n$.

They are shown in Figure 4 as dashed lines. It is found that $\Delta_d^{|M_J'|}$ is slightly smaller than $\Delta_m^{|M_J'|}$. The atomic alignment effect for $\sigma_{H,d}^{|M_J'|}$, $\sigma_{D,d}^{|M_J'|}$, and $\Delta_d^{|M_J'|}$ shows a similar tendency as that for $\Delta_m^{|M_J'|}$. The cross-section for the $M_J' = 0$ state is notably smaller than that for other $M_J' \neq 0$ states.

**4.2. Potential Energy Surface.** To understand the change of atomic alignment effect by dimer formation, we have to know about the potential energy surface (PES) for Ar ($^3P_2$) + $(CX_3CN)_n$. The PESs were roughly calculated using the ground state K atom instead of Ar ($^3P_2$) because it is difficult to obtain certain interaction energies by ab initio treatments of Ar ($^3P_2$) associated with highly excited states. The calculation was carried out by the Hartree−Fock method with the 6-31G basis set. The calculated model PESs for $CX_3CN$ and $(CX_3CN)_2$ are shown in Figure 5, panels A and B, respectively.

The PES is found to be attractive around the CN-group but repulsive around the $CH_3$-group for $CX_3CN$. For $(CX_3CN)_2$,

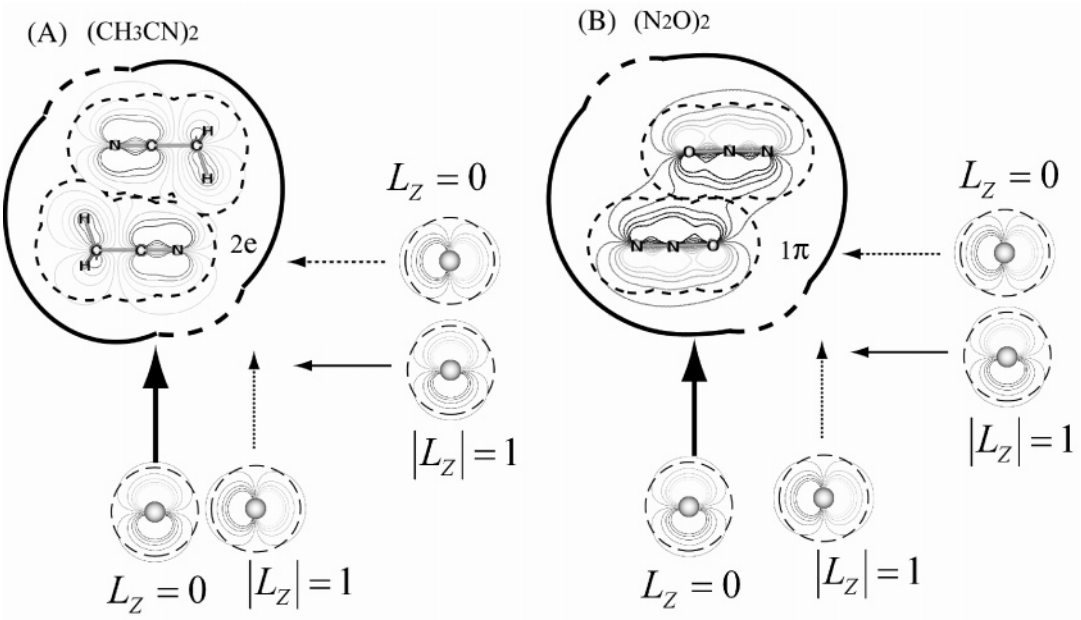


**Figure 6.** Schematic collisional configuration for Ar ($^3P_2$) + $(CX_3CN)_2$ (A) and for Ar ($^3P_2$) + $(N_2O)_2$ (B). The electron density distribution of the corresponding 2e orbital of $(CX_3CN)_2$ and the $1\pi$ orbital of $(N_2O)_n$ are shown. They were calculated using the GAUSSIAN 98 ab initio program package with the 6-311++G (3df, 2pd) basis set. The inner dashed lines express the van der Waals radius, and outer solid line and outer dashed lines schematically expresses the repulsive region and the attractive region, respectively. The thick arrow expresses the favorable collision. On the other hand, thin arrow expresses the unfavorable collision.

on the other hand, only a little region around the CN-group retains the attractive character, and the depth of the attractive well becomes shallow. The PES around the CN-group of one $CH_3CN$ component of dimer is found to be significantly perturbed by the $CH_3$-group of another $CH_3CN$. A similar perturbation on PES by dimer formation was observed for $(N_2O)_2$. As a reference, the PES for $(N_2O)_2$ is shown in Figure 5C.

**4.3. Reaction Process in the Dimer Reaction.** The reaction of Ar ($^3P_2$) + $CX_3CN$ is known as a dissociative energy transfer reaction. It has been confirmed that the energy transfer proceeds via the following electron-exchange process: (1) the electron in the relevant MO of the molecule transfers to the half-filled 3p orbital of Ar ($^3P_2$), then (2) the 4s electron of Ar ($^3P_2$) transfers to an empty Rydberg orbital of the molecule.

On the basis of the Mulliken approximation for the two electron integral,[24] the steric effect for the electron exchange can be approximated by the probability of orbital overlap.[25] In particular, we must consider the orbital overlap between the 3p orbital of Ar ($^3P_2$) and the MO of $CH_3CN$ ($CD_3CN$) in step 1 because step 2 is expected to be more isotropic than step 1.

There are two candidates for the possible pathways in the energy transfer processes of CN ($B^2\Sigma^+$) formation.

Path 1: $7a_1$ orbital → Rydberg orbitals $np\sigma$ and/or $nd\sigma$

Path 2: 2e orbital →
Rydberg orbitals $ns\sigma$, $np\sigma$, $np\pi$, and $nd\sigma$

From the perspective of the deuterium isotope effect on the atomic alignment effect, we recently tested the earlier proposal that the reaction of the 2e orbital (path 2) is responsible for the increase in the cross-section with deuteration, and we suggested that the expectation of the static anisotropy for the orbital overlap efficiency between the 2e orbital and the 3p orbital is inadequate to explain the deuterium isotope effect on both the atomic alignment and the molecular orientation dependence. In addition, it was suggested that the excited Rydberg states produced from the sideways collision is less efficient for the D-elimination as compared with those produced from the CN-end collision.

The dissociative energy transfer reaction of Ar ($^3P_2$) + $(CX_3CN)_2$ is also expected to proceed via the following similar two steps:

$$\text{Ar } (^3P_2) + (CX_3CN)_2 \rightarrow (CX_3CN)_2^{*}\cdots\text{Ar}$$

$$(CX_3CN)_2^{*}\cdots\text{Ar} \rightarrow \text{products} + \text{Ar}$$

The first step is the energy transfer process, and the second step is the dissociation process from the excited states. To understand the atomic alignment effect in the dimer reactions, we must take into account the atomic alignment effect in both steps. In general, it is likely that the dissociation dynamics is different for the monomer and the dimer because the excited-state produced by the energy transfer is different for the monomer and the dimer. Unfortunately, it is very difficult to discuss the atomic alignment effect in the dissociation process itself because the dissociation process from the excited-state of the dimer is an extremely complex process. However, we can expect that the dissociation process itself has little atomic alignment effect. For this reason, we confine our discussion to the qualitative one about the atomic alignment effect in the energy transfer process.

The perturbation of each $CX_3CN$ component due to dimer formation is expected to be small because the $CX_3CN$ dimer is bonded by a weak intermolecular force (binding energy ~0.2 eV).[26] The electron distribution for the MO of the monomer and for the corresponding MO of the dimer was calculated using the GAUSSIAN 98 ab initio program package with the 6-311G (3df, 2pd) basis set. The ab initio calculation of the dimer was carried out on the basis of the reported structure.[26] The calculated spatial distribution of the exterior electron on each $CX_3CN$ component in the corresponding MO of $CX_3CN$ dimer is almost the same as that of the monomer (see Figures 6 and 7). In other words, the MO of the $CX_3CN$ dimer can be approximated by a sum of the $7a_1$ or 2e orbitals of the $CX_3CN$ monomer. Therefore,

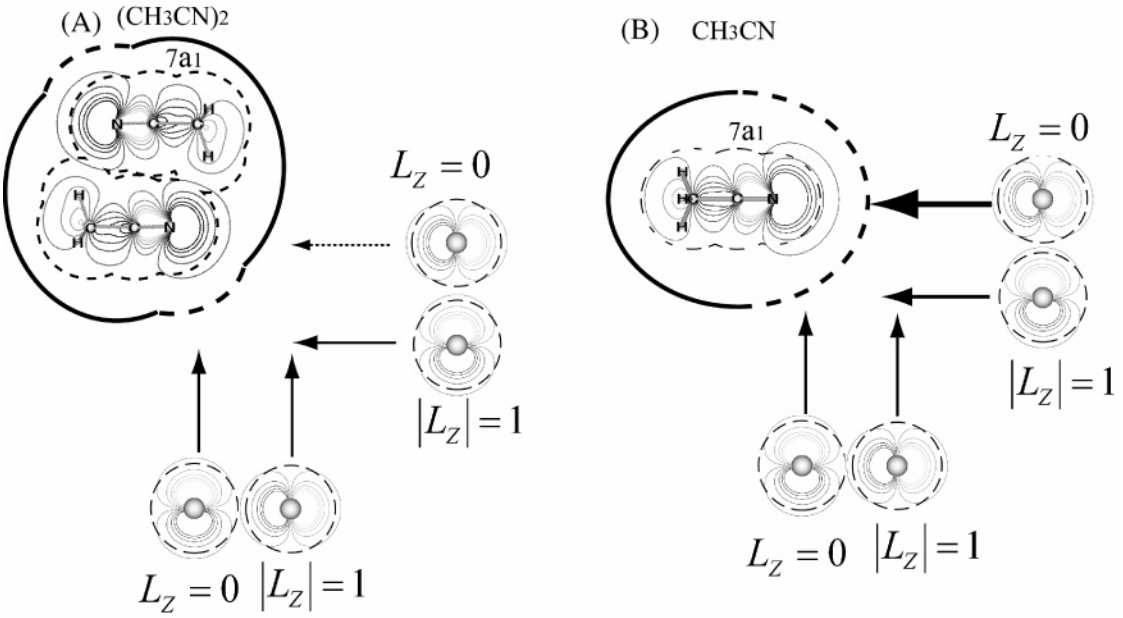


**Figure 7.** Schematic collisional configuration for Ar ($^3P_2$) + $(CH_3CN)_2$ (A) and for Ar ($^3P_2$) + $CH_3CN$ (B). The electron density distribution of the corresponding $7a_1$ orbital of $(CH_3CN)_2$ and $CH_3CN$ are shown. They were calculated by using the GAUSSIAN 98 ab initio program package with the 6-311++G(3df,2pd) basis set. The inner dashed lines express the van der Waals radius, and outer solid lines and outer dashed lines schematically express the repulsive region and the attractive region, respectively. The thick arrow expresses the favorable approach. On the other hand, thin arrow expresses the unfavorable approach.

we can estimate the steric effect for the dimer reaction as the orbital overlap efficiency between the 3p orbital of Ar ($^3P_2$) and the $7a_1$ or 2e orbital of each $CX_3CN$ component in the $(CX_3CN)_2$ dimer in consideration of the effect of dimer formation on PES.

**4.4. Atomic Alignment Effect in the $(CH_3CN)_2$ Dimer Reaction.** According to the previous study on the monomer reaction, it is unlikely that the 2e orbital (path 2) is responsible for the deuterium isotope effect in the reaction of $(CX_3CN)_2$.[23] At first, we tested this earlier proposal on the basis of the atomic alignment effect on the dimer reaction. As shown in Figure 5, the PES for $(CH_3CN)_2$ is analogous with that for $(N_2O)_2$. Moreover, the spatial distribution of the 2e orbital of $CH_3CN$ is also analogous with the $1\pi$ orbital of $N_2O$. From this point of view, it is reasonable to assume that the atomic alignment effect for path 2 in the reaction of $(CH_3CN)_2$ is analogous with that for $(N_2O)_2$. For the $(N_2O)_2$ reaction, we observed a significant decrease of $\sigma_d^{|2|}$ and $\sigma_d^{|1|}$ relative to $\sigma_d^0$ such that $\sigma^0/\sigma^{|1|}/\sigma^{|2|} = 0.81/0.44/0.49$.[15] As shown in Figure 6, on the basis of the efficiency of the orbital overlap between the $1\pi$ orbital with the atomic 3p orbital, the configuration of $L_Z = 0$ is favorable for the collision from the sideways direction with a small impact parameter, whereas the $|L_Z| = 1$ configuration is favorable for the collision from the molecular axis with a large impact parameter. Because dimer formation dramatically decreases the attractiveness of the PES, the reactivity of the $|L_Z| = 1$ configuration with a large impact parameter should become small. This expectation is in good agreement with the drastic change of the atomic alignment effect in the $(N_2O)_2$ reaction by dimer formation. An analogous expectation should be valid for path 2 in the reaction of $(CX_3CN)_2$. However, in contrast with this expectation, we observed a significant decrease of $\sigma^0_{H(D),d}$ relative to $\sigma^{|1|}_{H(D),m}$ and $\sigma^{|2|}_{H(D),m}$ for the reaction of $(CX_3CN)_2$. Therefore, it is unlikely that the 2e orbital (path 2) is responsible for the enhancement in the cross-section with deuteration in the reaction of $(CX_3CN)_2$. We strongly suggest that the deuterium isotope effect on the steric effect is attributable to the competition between the CN ($B^2\Sigma^+$) formation from the different excited states that are characterized as the excitation from the same $7a_1$ orbital to the different Rydberg orbital (path 1). As shown in Figure 7, on the basis of this assumption, a significant decrease of the reactivity at the $L_Z = 0$ configuration by dimer formation is expected for the collisions from the CN-end direction because the PES around the CN-group of the dimer is significantly perturbed by the $CH_3$-group of another $CH_3CN$. In particular, the collision from the direction of C−N axis is obstructed by the repulsive wall from the $CX_3$-group of another $CX_3CN$ component. For the collisions from the sideways direction, on the other hand, the influence exerted by dimer formation is expected to be reduced because such collisions take place apart from the $CX_3$-group. Therefore, we can expect a notable decrease of the reactivity for the $L_Z = 0$ configuration as compared with that for the $|L_Z| = 1$ configuration. This expectation is consistent with the notable decrease of $\sigma^0_{H(D),d}$ relative to $\sigma^{|1|}_{H(D),m}$ and $\sigma^{|2|}_{H(D),m}$ in the reaction of $(CX_3CN)_2$. In other words, the dimer formation decreases the contribution from the CN-end collision relative to that from the sideways collision.

In our previous report,[23] we proposed that the excited Rydberg states produced from the sideways collision are less efficient for the D-elimination as compared with those produced from the CN-end collision. On the basis of this assumption, the atomic alignment dependence of the $(CH_3CN)_2$ reaction should resemble that of $(CD_3CN)_2$. This expectation is confirmed by the experimental atomic alignment effect for the dimer reaction. In addition, the similarity between $\sigma^{|Mj|}_{H,d}$ and $\Delta^{|Mj|}_m$ might indicate that dimer formation disturbs the H-elimination process in the excited Rydberg states produced from the sideways collision and enhances the branching to the CN ($B^2\Sigma^+$) formation channel.

As a whole, the effects of dimer formation on both the atomic alignment dependence and the deuterium isotope effect are well supported by the following suggestions previously reported in the $CX_3CN$ monomer reaction.[23]

(1) The deuterium isotope effect is attributed to the competition of the CN ($B^2\Sigma^+$) formation from the different excited states

that are characterized as the excitation from the same $7a_1$ orbital to the different Rydberg orbital (path 1).

(2) The formation of excited Rydberg states (step 2 in the electron-exchange process) is selected by the mutual configuration between the molecular orientation and the atomic alignment in the collision frame.

(3) The excited Rydberg states produced from the sideways collision are less efficient for the D-elimination as compared with those produced from the CN-end collision.

From a series of studies, we strongly suggest that the selection of the final excited-state via the electron exchange process (corresponding to the transfer of the 4s electron of Ar ($^3P_2$) to an empty Rydberg orbital of the molecule) is controlled by the mutual configuration between the molecular orientation and the atomic alignment in the collision frame with a significant spin interaction between the unpaired inner orbital and the outer extended orbital.

## References and Notes

(1) Marcus, R. A. *Angew. Chem., Int. Ed. Engl.* **1993**, *32*, 1111.
(2) Gundel, L. A.; Setser, G. W.; Clyne, M. A. A.; Coxon, J. A.; Nip, W. *J. Chem. Phys.* **1976**, *64*, 4390.
(3) Velazco, J. E.; Kolts, J. H.; Setser, D. W. *J. Chem. Phys.* **1978**, *69*, 4357.
(4) Balamuta, J.; Golbe, M. F. *J. Chem. Phys.* **1982**, *76*, 2430.
(5) DeVries, M. S.; Tyndall, G. W.; Cobb, C. L.; Martin, R. M. *J. Chem. Phys.* **1986**, *84*, 3753.
(6) Johnson, K.; Pease, R.; Simons, J. P. *Mol. Phys.* **1984**, *52*, 955.
(7) Ohoyama, H.; Kasai, T.; Ohashi, K.; Kuwata, K. *Chem. Phys. Lett.* **1987**, *136*, 236.
(8) Ohoyama, H.; Iguro, T.; Kasai, T.; Kuwata, K. *Chem. Phys. Lett.* **1993**, *209*, 361.
(9) Ohoyama, H.; Kawaguchi, H.; Yamato, M.; Kasai, T.; Brunetti, B. G.; Vecchiocattivi, F. *Chem. Phys. Lett.* **1999**, *313*, 484.
(10) Yamato, M.; Okada, S.; Wu, V. W. −K.; Ohoyama, H.; Kasai, T. *J. Chem. Phys.* **2000**, *113*, 6673.
(11) Yamato, M.; Ohoyama, H.; Kasai, T. *J. Phys. Chem. A* **2001**, *105*, 2967.
(12) Okada, S.; Ohoyama, H.; Kasai, T. *J. Chem. Phys.* **2003**, *119*, 7131.
(13) Watanabe, D.; Ohoyama, H.; Matsumura, T.; Kasai, T. *J Chem. Phys.* **2006**, *125*, 084316.
(14) Percival, I. C.; Seaton, M. J. *Proc. Cambridge Philos. Soc.* **1957**, *53*, 654.
(15) Watanabe, D.; Ohoyama, H.; Matsumura, T.; Kasai, T. *J Chem. Phys.* **2006**, *125*, 224301.
(16) Kasai, T.; Che, D. C.; Ohashi, K.; Kuwata, K. *Chem. Phys. Lett.* **1989**, *163*, 246.
(17) Che, D. C.; Kasai, T.; Ohoyama, H.; Ohashi, K.; Fukawa, T.; Kuwata, K. *J. Phys. Chem.* **1991**, *95*, 8159.
(18) Kanda, K.; Igari, N.; Kikuchi, Y.; Kishida, N.; Igarashi, J.; Katsumata, S. *J. Phys. Chem.* **1995**, *99*, 5269.
(19) Tabayashi, K.; Shobatake, K. *J. Chem. Phys.* **1987**, *87*, 2404.
(20) Sadeghi, S.; Setser, D. W. *Chem. Phys. Lett.* **1981**, *82*, 44.
(21) Bourene, M.; LeCalve, J. *J. Chem. Phys.* **1973**, *58*, 1452.
(22) Kanda, K.; Nagata, T.; Ibuki, T. *Chem. Phys.* **1999**, *243*, 89.
(23) Matsumura, T.; Ohoyama, H.; Watanabe, D.; Yasuda, K.; Kasai, T. *J. Phys. Chem. A* **2007**, *111*, 3069.
(24) Mulliken, R. S. *J. Chim. Phys. Phys. Chim. Biol.* **1949**, *46*, 497.
(25) Ohno, K. *Bull. Chem. Soc. Jpn.* **2004**, *77*, 887.
(26) Lego, E. M. C-.; Ramon, J. M. H-.; Gallego, A. P-.; Nunez, E. M-.; Ramos, A. F-. *J. Mol. Struct.* **2000**, *498*, 21.